

## Supplementary Information to “A phase-field model for the evaporation of thin film mixtures”

Olivier J.J. Ronsin, DongJu Jang, Hans-Joachim Egelhaaf, Christoph J. Brabec and Jens Harting

### Parameter choice for the investigation of the evaporation kinetics at low evaporation rates

In order to investigate the drying kinetics of our phase-field model in the low-Biot regime, we investigate the impact of the phase change parameters, the driving force  $F_k$  and the energy barrier  $H$  on the drying kinetics. Four parameter sets are chosen, for which the free-energy dependence on the order parameter is shown in Figure 1. The two parameter sets used for Figure 3 in the main text correspond to the blue and red curves in the figure below.

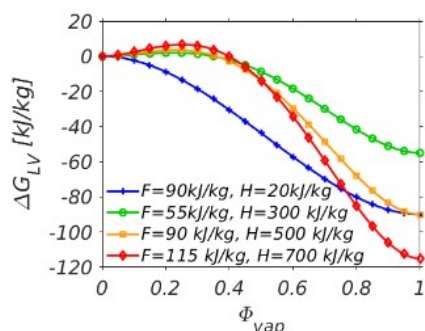


Figure 1: Order parameter dependence of the free energy for the four tested parameter sets.

### Influence of model parameters on the drying rate

The figure below shows the impact of the model parameters on the interface velocity  $V_{int,0}$ , which is evaluated at the beginning of the drying for very high solvent volume fraction (90%). The interface velocities vary linearly with the driving force of the solvent evaporation  $F_{solv}$  (Figure 2a) and decrease when the energy barrier increases. If the driving force is low and the energy barrier is sufficiently high, the vapor phase can become unstable and disappear, depending on the surface tension and its initial size in the simulation. Figure 2b shows that the interface velocity is proportional to the Allen-Cahn mobility coefficient.

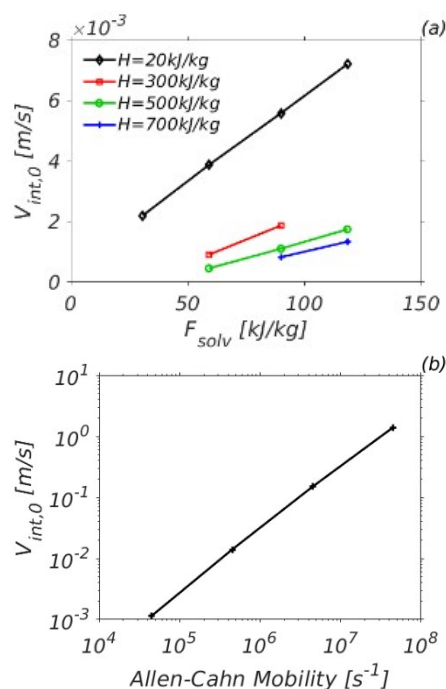


Figure 2: Effect of the driving force of the solvent evaporation (a) and of the Allen-Cahn mobility (b) on the initial evaporation rate.

As pointed out before, the intensity of the solvent flow at the boundary has a strong impact on the solvent concentration field (the solvent volume fraction remains high if the flux is low, but air can enter in the liquid film if the flow is too strong). However, the velocity of the interface varies logarithmically with the flux which leads to a weak sensitivity to this parameter (compared to the sensitivity to the driving force for the solvent and the Allen-Cahn mobility, see Figure 2), namely a 50% variation over 3 decades. The evaporation rate decreases with increasing flux, simply because there is more residual air in the film. This shows clearly that in our model the evaporation is mainly due to the phase change at the film surface as desired, and not due to diffusion. The effect of the “air evaporation driving force”, which is a purely adjustable parameter, can be understood in the same way: the larger this parameter is, the less air remains in the film, and the higher becomes the evaporation rate. It can be seen in Figure 3b that the drying rate becomes insensitive to this parameter at high  $F_{air}$ .

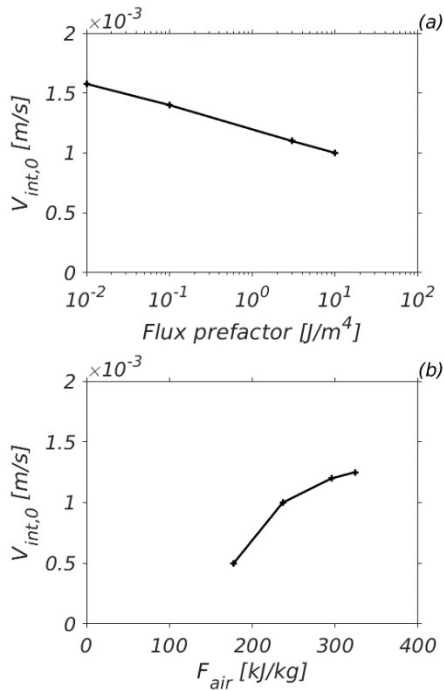


Figure 3: Effect of the solvent outflow (a) and of the air evaporation driving force (b) on the initial evaporation rate.

#### Drying kinetics of the two-solvent system

Figure 4 shows the time-dependent mean volume fraction for both solvents in the film corresponding to the fields shown in Figure 6 of the main text.

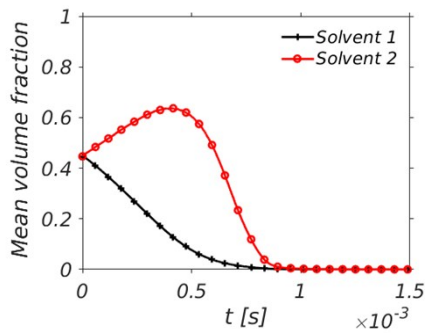


Figure 4: Time-dependent mean solvent volume fraction in the liquid film.

Figure 5 shows the time-dependent interface velocity for the two-solvent system. We expect then the global drying rate to be roughly  $V_{int1} \cdot \phi_1 + V_{int2} \cdot \phi_2$ , but this is not the case. The global drying rate is much closer to the product of the average drying rate of both solvents with the global volume fraction.

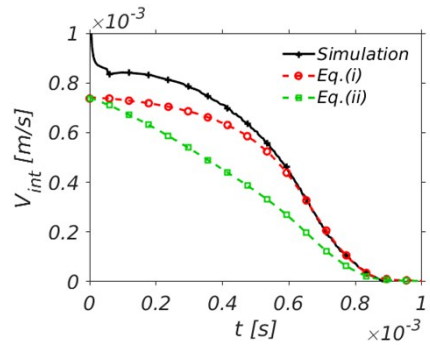


Figure 5: Simulated and modelled instantaneous evaporation rate, Eq.(i) is  $(\phi_1 + \phi_2)(V_{int1} + V_{int2})/2$  and Eq.(ii) is  $V_{int1} \cdot \phi_1 + V_{int2} \cdot \phi_2$